THE LONG-TERM COURSE OF THE ANNUAL TOTAL SUNSHINE DURATION IN EUROPE AND CHANGES IN THE PHASES OF THE THERMOHALINE CIRCULATION IN THE NORTH ATLANTIC (1901–2018)

ANDRZEJ A. MARSZ [1], ANNA STYSZYŃSKA [2], DOROTA MATUSZKO [3]

[1] Polish Geophysical Society, Baltic Branch, Gdynia, Poland
[2] Association of Polish Climatologists, Warszawa, Poland
[3] Institute of Geography and Spatial Management, Jagiellonian University, Kraków, Poland

Manuscript received: October 30, 2022
Revised version: March 31, 2023

MARSZ A.A., STYSZYŃSKA A., MATUSZKO D., 2023. The long-term course of the annual total sunshine duration in Europe and changes in the phases of the thermohaline circulation in the North Atlantic (1901–2018). *Quaestiones Geographicae* 42(3), Bogucki Wydawnictwo Naukowe, Poznań, pp. 49–65. 9 figs, 3 tables.

ABSTRACT: The current study was based on sunshine duration data from 13 European stations during 1901–2018. It was found that the variability in the annual total sunshine duration (SD) over Europe is related to the variability in the component of the surface thermohaline circulation in the North Atlantic (NA THC). Positive NA THC phases (the condition of the 'warm' North Atlantic) correspond to the periods of increased SD (brightening), while negative phases correspond to the periods of decreased SD (dimming). These relationships remain stable and statistically significant. The mechanism of these relationships is based on the influence of weakened or enhanced heat flow from the ocean to the atmosphere on the course of the mid-tropospheric circulation processes. In periods of positive thermohaline circulation in the North Atlantic (NA THC) phases, the share of long waves (macrotype W according to the Wangengejm–Girs classification) increases, with the occurrence of which the frequency of anticyclonic weather over Europe increases, whereas in the periods of negative NA THC phases, the share of shorter waves (macrotypes E and C) increases, with the occurrence of which the frequency of cyclonic (frontal) weather over Europe increases. It is characterised by increased layer cloud cover, limiting the SD. Thus, along with changes in the thermal condition of the North Atlantic, the structure of cloud cover over Europe changes and becomes a factor regulating long-term changes in the annual total SD.

KEY WORDS: sunshine duration, North Atlantic thermohaline circulation, mid-tropospheric circulation, brightening, dimming, Europe

Corresponding author: Dorota Matuszko; d.matuszko@uj.edu.pl

Introduction

The long-term course of the annual total sunshine duration (SD) in Europe shows variability in the occurrence of successive long-term brightening and dimming (e.g. Brázdil et al. 1994, Sanchez-Lorenzo et al. 2008, 2009, Manara et al. 2015). Until now, long-term variability in the course of the SD over Europe was most often explained as a result of changes in the concentration of aerosols of natural and/or anthropogenic origin (e.g. Liepert 2002, Norris, Wild 2007, Ruckstuhl, Norris 2009, Vetter, Wechsung 2015), and less often as the influence of atmospheric

https://doi.org/10.14746/quageo-2023-0023
ISSN 2082-2103, eISSN 2081-6383

circulation (e.g. Sanchez-Lorenzo et al. 2008, Stjern et al. 2009).

The relatively close relationship between changes in the annual SD in Central Europe and long-term changes in mid-tropospheric circulation was pointed out by Marsz et al. (2022). According to their research, changes in the structure of the mid-tropospheric macrocirculation processes that create circulation epochs (Girs, Kondratovich 1978) are controlled by changes in the intensity of the surface component of the thermohaline circulation in the North Atlantic (North Atlantic Thermohaline Circulation [NA THC]; Meridional Overturning Circulation [AMOC]). Therefore, the annual total SD in Central Europe change in line with the changes in NA THC phases. Previous studies have shown that in the years 1951–2018, positive NA THC phases corresponded to the periods of increased SD, while negative phases corresponded to the periods of decreased SD (Marsz et al. 2022).

To determine the nature of the variability in the SD and to explain its causes, the analysis of long-term components seems to be the most important. The aim of this study is to identify common features of the long-term course of the annual total SD at the European stations with the longest measurement series and to explain the relationships between the variability in the intensity of thermohaline circulation in the North Atlantic (NA THC) over a period of over 100 years (1901–2018) and SD. This issue was described for a shorter period (1951–2015) in the work of Marsz et al. (2022), and this article attempts to answer the following questions:

1. Are the relationships between changes in NA THC intensity and annual total SD which were described in the work of Marsz et al. (2022), also found in older, pre-1951 parts of the series, i.e. are the relationships stable over time?
2. Do long-term changes in the SD in Europe show direct relationships with changes in the temperature of the surface of the North Atlantic (hereinafter sea surface temperature, SST), and if so, what is the spatial distribution of water bodies on which the variability in SST shows direct relationships with SD?

Data

In view of the large diversity in the date of the beginning of the measurements of SD at individual stations and the number of measurement breaks, it was assumed that the analysed time series must cover a uniform period from 1901 to 2018, and the number of shortages in measurement series during this period cannot exceed 1 annual value. In this analysis, it was decided not to consider heliographic sequences from high mountain stations because of the specific SD forming over them, especially in winter

Table 1. Stations used in the study.

No.	Station	Country	Geographical coordinates	Altitude (m a.s.l.)	Number of supplementations of annual mean values	Data source
1	Armagh	GB	54.35°N, 6.65°W	62	0	Met Office
2	De Bilt	NL	52.10°N, 5.18°E	1	1 (1945)	ECAD
3	Geneva	CH	46.20°N, 6.15°E	405	0	ECAD
4	Basel	CH	47.53°N, 7.58°E	316	0	HISTALP
5	Zurich	CH	47.38°N, 8.57°E	555	0	ECAD
6	Copenhagen	DK	56.68°N, 12.53°E	9	0	DMI
7	Potsdam	DE	52.38°N, 13.06°E	81	1 (1945)	DWD
8	Kremsmunster	AT	48.06°N, 14.13°E	382	0	HISTALP
9	Klagenfurt	AT	46.65°N, 14.32°E	459	0	HISTALP
10	Zagreb	HR	45.82°N, 15.97°E	157	1 (1921)	HISTALP
11	Vienna	AT	48.25°N, 16.36°E	209	0	HISTALP
12	Wroclaw	PL	51.10°N, 16.90°E	120	0	Bryś (2013), Marsz et al. (2021)
13	Krakow	PL	50.07°N, 19.97°E	206	0	IGiGP UJ

Note: State affiliation of the station according to the ISO 316 code, DMI (https://www.dmi.dk/vejrarkiv/maned-ens-sasonens-og-arets-vejr/tekst-kort-og-nogletal-maned/), DWD (https://www.dwd.de/EN/climate_environment/cdc/cdc_node_en.html), ECAD (https://www.ecad.eu/), HISTALP (http://www.zamg.ac.at/histalp/), IGiGP UJ – Institute of Geography and Spatial Management, Jagiellonian University in Kraków, Met Office (https://www.metoffice.gov.uk/).

months (Urban et al. 2018, Bartoszek et al. 2021). As a result of a detailed survey of SD measurement data at European stations, 13 stations were found (Table 1). The few missing annual values were calculated by completing monthly values (De Bilt) or by calculating the annual value as an average of the year preceding and the year following the year with no data (Potsdam, Zagreb).

The data used to analyse the relationship between the spatial distribution of annual SST values in the North Atlantic and the annual SD in Europe and to calculate the value of the DG_{3L} index, characterising the NA THC intensity, is the set of monthly SST values derived from the ERSST v.3b set (NOAA Extended Reconstructed Sea Surface Temperature; Smith et al. 2008). This set is based on SST measurements *in situ*, performed from research vessels and buoys compiled in the ICOADS R2.5 database (The International Comprehensive Ocean-Atmosphere Data Set). It is a global set with a spatial resolution of 2° × 2° and a monthly temporal resolution. The monthly SST averages in this set are considered reliable since 1880 and highly reliable since 1950 (Smith et al. 2008). The data were downloaded from NOAA/OAR/ESRL PSL, Boulder, CO, USA, from their Web site at https://psl.noaa.gov/data/gridded/data.noaa.ersst.v3.html.

The index marked with the acronym DG_{3L} (the Delta of Gulf Stream, 3 years) characterises the relative amount of heat transferred with the transport of water by NA THC from the tropical North Atlantic region to the north. A detailed description of the physical foundations of this index and its structure is explained in the works of Marsz (2015) and Wrzesiński et al. (2019). The value of the DG_{3L} index is a standardised anomaly, which indicates the extent to which the flux of the heat transported by THC in the North Atlantic is greater or less than the 1901–2000 average.

In the course of the DG_{3L} index, next to the strong inter-annual variability (Fig. 1), very strong long-term (multi-decadal) variability is marked, creating clear periods in which the value of this index is, on average, lower or higher than zero. This corresponds to the periods of weakening and strengthening of the surface intensity of the NA THC component, in which the northward flow of heat is below the average for the century and above this average. This makes it possible to separate out long-term negative and positive phases in the course of NA THC. The boundaries of the phases are determined by the transition of the DG_{3L} index value through zero.

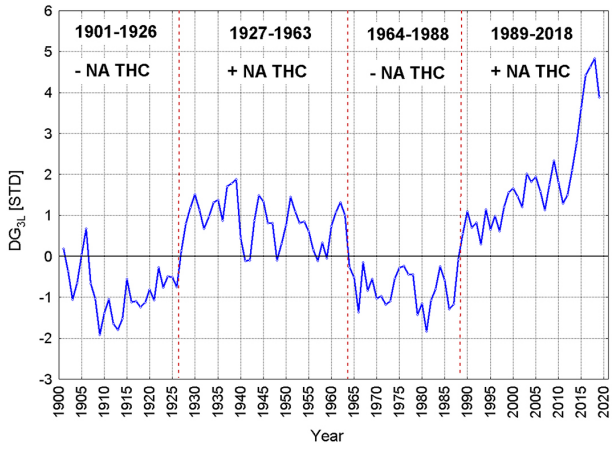

Fig. 1. Course of the DG_{3L} index in the years 1901–2018. Marked boundaries of negative and positive North Atlantic Thermohaline Circulation phases.

It should be noted that the course of the DG_{3L} index in the last positive phase of NA THC (1989–2018) differs significantly from the course in the earlier phases; from the beginning of this phase, its values never drop below zero, and in its course, there is a positive trend, strongly increasing since 2011. In the period under consideration, 1901–2018, there were four distinct phases in the course of NA THC, differing in length, mean values of the index and their variability ranges (Table 2), with the first two-part negative NA THC phase beginning earlier than in 1901 (in 1873) and the last warm phase (1989–…) continuing until today.

Table 2. Characteristics of the DG_{3L} index in the North Atlantic Thermohaline Circulation phases occurring in the years 1901–2018.

North Atlantic Thermohaline Circulation Phases	Years	Duration (years)	DG_{3L} index			
			Average	Min	Max	STD
1	1901–1926	26	−0.846	−1.921	0.682	0.605
2	1927–1963	37	0.844	−0.116	1.879	0.563
3	1964–1988	25	−0.782	−1.836	−0.073	0.472
4	1989–2018	31	1.851	0.299	4.836	1.226

Additionally, the work uses time series of the geopotential height of the isobaric surface of 500 hPa (h500) and similar series of pressure at sea level (SLP) with monthly resolution from selected grids. The annual values of h500 and SLP for individual grids were calculated as simple arithmetic means of monthly values in a given calendar year. Both types of data come from National Centers for Environmental / National Center for Atmospheric Research (NCEP/NCAR) Reanalysis (Kalnay et al. 1996) and were downloaded from NOAA/OAR/ESRL PSL, Boulder, CO, USA, from their Web site at https://psl.noaa.gov/data/gridded/data.ncep.reanalysis.pressure.html. The period covered by these data is shorter (1949–2018) than the basic analysis period in this work.

Research methods

The time series of the annual total SD from the years 1901–2018 from 13 stations is given in Table 1. From the values of all series, the area average series of the annual total SD was calculated as arithmetic means. This series is marked as SD_{13S} (**S**unshine **D**uration, 13 stations).

The courses of all variables (series of the SD at individual stations), except for one case (Copenhagen & Zagreb), are significantly correlated with each other, the vast majority of which variables are highly significant (p <0.001). This justifies analysing the set using the factor analysis method. It makes it possible to explain the total stock of variance contained in the set of the annual total SD at the analysed stations and, as a result of further analyses, to explain the activity of which factors this variance is related to. For the factor analysis, raw series of the annual total SD at individual stations, counted in hours, were adopted, without transforming them into anomalies, without standardisation, and without smoothing them using any filters.

The results of the factor analysis revealed the existence in the set of three principal components (PC) of eigenvalues greater than 1.0, which are statistically significant according to the Kaiser criterion. Similarly, the scree test (Hill, Lewicki 2007) indicated that the first three factors (PC) sufficiently explain the variance of the analysed set of variables. The selected three factors together explain 73.59% of the total variance of the set, of which:

- the first principal component (PC1) with an eigenvalue of 6.99 explains 53.78%,
- the second principal component (PC2) with an eigenvalue of 1.52 explains 11.67% and
- the third principal component (PC3) with an eigenvalue of 1.06 explains 8.13% of the total variance.

The analysis of the relationships between the time series of factor values of each PC (eigenvectors) and the series of SD at individual stations made it possible to explain the physical meaning of individual distinguished PC.

The SD at all stations shows highly significant (p <<0.000) positive correlations with 1 eigenvector (PC1). This vector presents standardised anomalies of the average annual SD from the 13 analysed stations in individual years. The correlation coefficient (r) between PC1 and the course of SD_{13S} is 0.999. The relationship is as follows:

$$SD_{13S} = 1696.9(\pm 0.6) + 124.5(\pm 0.6) \times PC1.$$

This almost completely (adj.R^2 = 0.997) explains the variability in SD_{13S} in the area under consideration. The variability included in the courses of SD_{13S} and PC1 is identical, and the two courses only differ in the scaling of the y-axis (Fig. 2).

This allows us to interpret that PC1, explaining more than half of the total variance of the SD set at all analysed stations, presents a common variability occurring in their series. Thus, the same percentage of the total variance (53.78%) of

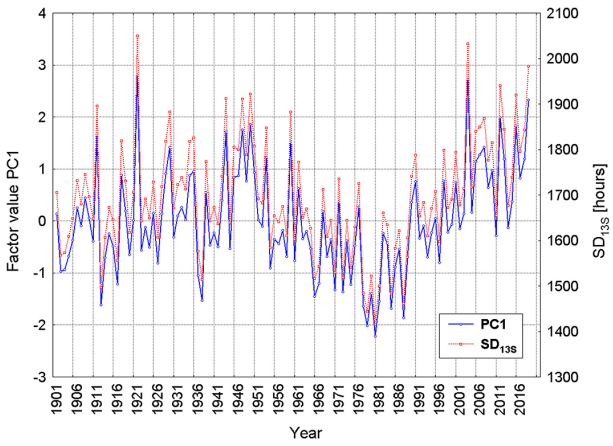

Fig. 2. Time series of SD_{13S} and the factor values of the first PC of this set (eigenvector PC1). PC, principal components; SD, sunshine duration.

the annual SD must be represented by area-average (SD_{13S}).

The results of the PC analysis allow for the conclusion that in the considered set of European stations with very different locations, more than half of the common variability occurs in their course of SD. The second and third eigenvectors, explaining about 20% of the variance, show the features of regional differentiation in the SD in the area of the considered part of Europe.

For the analysis of the relationships between the variability in the area-average annual SD in Europe (SD_{13S}) and the variability in the NA THC intensity (DG_{3L}), standard statistical procedures were used, mainly linear correlation analysis and regression analysis. The statistical significance of certain relationships was tested by means of tests appropriate for a given procedure (tests of differences between averages, t and F tests, etc.).

The analysis of relationships between SD_{13S} with SST in the North Atlantic was performed, correlating the annual SST series in nodal points (grids) with a spatial resolution of 10° x 10°λ counted every 10° (70°N, 10°E; 70°N, 000°; 60°N, 000°; 60°N, 10°W;...). Between the values of the correlation coefficients at nodal points, an interpolation using the ordinary kriging method was carried out, resulting in a spatial distribution (map) of isocorrelates, spanning on the surface of the North Atlantic between 20°N and 70°N and between 80°W and 10°E.

Results

Relationships between the NA THC phases and the average annual SD at European stations

In the years 1901–2018, the SD_{13S} is characterised by a significant inter-year and a long-term variability, with the long-term average value of SD_{13S} amounting to 1,696.9 h and the standard deviation being 124.6 h. Additionally, in the SD_{13S} series, there is a strong autocorrelation; the analysis of partial autocorrelations shows the presence of a statistically significant autocorrelation for four consecutive years, indicating that the annual SD in Europe changes under the influence of a factor(s) with significant inertia.

In the multi-year period 1901–2018, there is a highly significant positive correlation (r = 0.50, $p << 0.001$) between the course of the SD_{13S} and the DG_{3L} index, explaining that the variability in NA THC is determined by (r^2) 25% of the common variance in the SD at European stations. A change in the value of the DG_{3L} index by 1 unit entails a change in the annual SD by 46.8 (± 7.5) h. With the variability in the DG_{3L} index in the range from –2 to +4.5, it gives a variability in SD_{13S} by approximately 300 (±15) h, which is more than twice the standard deviation of SD_{13S}.

The scatterplot of points in the common space of DG_{3L} and SD_{13S} (Fig. 3) reveals that the relationship is far from strict. The asymmetry of the concentration of empirical points above and below the regression line is noticeable; points above this line show a much larger dispersion. The revealing 2 years with significantly different values from the rest of the population, with SD_{13S} exceeding 2,000 h (1921 and 2003), significantly weaken the strength of the relationship. Checking these values against the other series, not included in this study (Lindenberg, Jena [DE]; Durham, Bradford [GB]; Maastricht [NL]), makes it possible to conclude that the years actually mentioned were characterised in Europe by an anomalously high SD (related to an anomalously low cloud cover in those years).

The division of the entire 118-year series of SD_{13S} values for the time periods corresponding to the distinguished NA THC phases (Table 2) and the calculation of SD_{13S} mean values in individual periods (Table 3) show the existence of a clear diversity of the annual SD over Europe referring

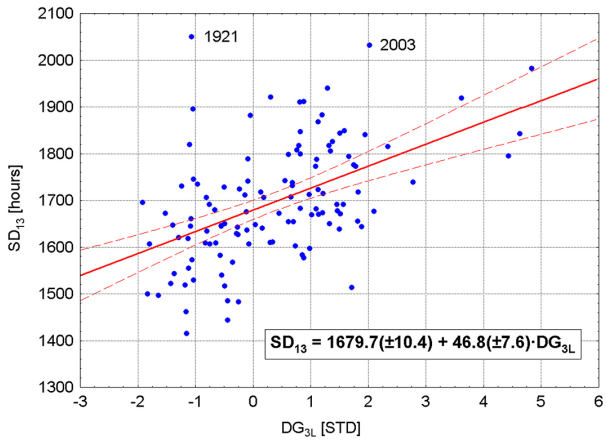

Fig. 3. Relationship between the DG_{3L} index and SD_{13S}, 1901–2018. SD, sunshine duration.

Table 3. Average values of the annual area sunshine duration over Europe (SD13S) and the ranges of their variability in the subsequent North Atlantic Thermohaline Circulation phases.

North Atlantic Thermohaline Circulation phase	Years	Duration (years)	SD_{13S} (h)			
			Average	Min	Max	Median
1	1901–1926	26	1,681.7	1,497.0	2,050.2	1,661.2
2	1927–1963	37	1,730.1	1,514.2	1,921.7	1,718.1
3	1964–1988	25	1,575.7	1,415.9	1,735.2	1,582.9
4	1989–2018	31	1,770.0	1,597.1	2,032.3	1,759.0

to the NA THC phases. The periods of increased SD, corresponding to the phases of brightening, are associated with the occurrence of the positive NA THC phase, while the periods of reduced SD corresponding to the phases of dimming are associated with the occurrence of the negative NA THC phase.

Differences between average SD_{13S} for the periods 1927–1963 and 1964–1988 as well as 1964–1988 and 1989–2018 are highly significant ($p << 0.001$). The difference between the averages for the periods 1901–1926 and 1927–1963 is statistically significant, but only at the level of 0.05. One of the reasons for such a low significance of the difference between these periods is the presence of two strong outliers in the period 1901–1926 (in 1911, SD_{13S} = 1,874 h, and in 1921, SD_{13S} = 2,050 h), with the SD recorded in 1921 being the maximum SD_{13S} value throughout the 118-year observation period.

The analysis of the cross-correlation between the DG_{3L} index (antecedent variable) and SD_{13S} (delayed variable) shows that the relationships

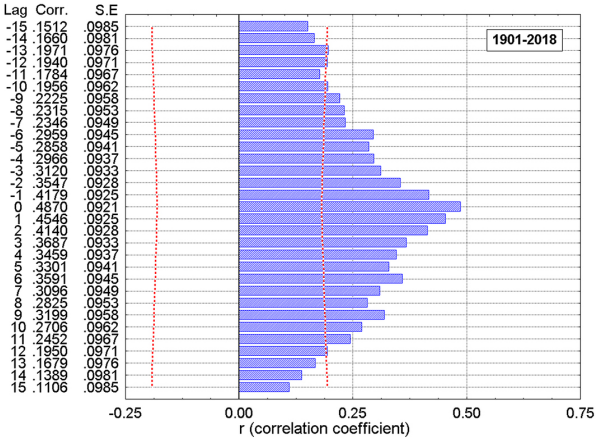

Fig. 4. Cross-correlations between the DG_{3L} index (antecedent variable) and sunshine duration SD_{13S} (delayed variable). Graded curves – the range of ± standard errors SE that sets the limits of statistical significance p = 0.05 of a correlation. Correlated series 1901–2018.

between these values are not limited to synchronous relationships but also have a very strong inertial component (Fig. 4). Significant correlations between these values range from −9 years to 11 years, reaching the maximum strength of the relationship in a year with the zero time shift. This shows that the earlier thermal condition of the ocean, governed by the variability in NA THC, affects the SD_{13S}. Thus, the value of the DG_{3L} index from the previous year explains 19.5% of the SD_{13S} variance in a given year, the value of the DG_{3L} index from 2 years ago explains 15.8% of the SD_{13S} variance, and the value of the DG_{3L} index from 3 years ago explains ~14.2% of the SD_{13S} variance in the given year.

The reasons for the delays in the reaction of SD to changes in the intensity of NA THC are manifold. The most important role in the formation of these delayed relationships is played by the great thermal inertia of the ocean and the very slow propagation of water with increased or decreased amounts of heat transported by NA THC, which is then reflected in the nature of the mid-tropospheric circulation, controlled by changes in the location of heat flows from the ocean to the atmosphere (Marsz et al. 2022). Certainly, the structure of the DG_{3L} index has a significant impact on the formation of time shifts, which constitutes the weighted SST value over 3 consecutive years.

There is a very strong autocorrelation in the DG_{3L} index series. As a result, it is impossible to create a multiple regression linear equation in which SD_{13S} would be a function of the DG_{3L} index from year k and earlier (k-1, k-2, ...) values of this index. The analysis of non-linear relationships shows that earlier changes in the DG_{3L} index have a significant impact on the value of the SD up to 4 years, and the impact is complicated. The strongest increase in SD_{13S} in year k is when the DG_{3L} index in year (k-1) is positive, and in the following year, the (k) value of the index will increase significantly in relation to the previous value.

Relationships between the SST field in the North Atlantic and area SD in Europe

In the course of SST in the North Atlantic, there is a strong and distinct multi-decadal variability, which has been repeatedly analysed and described in the literature (e.g. Kushnir 1994, Delworth, Greatbatch 2000, Dong, Sutton 2005, Dima, Lohmann 2007, Sutton, Dong 2012). The surface component of the thermohaline circulation controls a large percentage of this long-term variability in SST in the North Atlantic. For this reason, between the AMO index (Atlantic Multidecadal Oscillation; Kerr 2000, Enfield et al. 2001), which characterises the thermal state of the entire North Atlantic (between 0° and 80°N and 80°W and 0°), and the DG_{3L} index, there are statistically significant relationships. The value of the correlation coefficient between the DG_{3L} index and the AMO unsmoothed index (AMO unsmooth, long; https://climatedataguide.ucar.edu/climate-data/atlantic-multi-decadal-oscillation-amo) is equal to 0.67 and is highly significant (p <0.001, 1901–2018). Despite the generally similar nature of both indices, namely, AMO and DG_{3L}, the variability in the AMO index explains only ~8% of the variance of SD_{13S}, while the variability in the DG_{3L} index explains ~25% of the variance of the average annual SD in Europe over a period of 118 years.

The discovered relationships between the course of SD_{13S} and the NA THC phases raise the question whether there are any direct relationships between the variability in SST in the North Atlantic and SD_{13S} in the considered multi-year period, and if so, how are they formed. One of the important issues is the answer to the question whether SD shows any relationships with the variability in SST across the North Atlantic, consistent with the variability in AMO, or whether the strength of these relationships is varied in space along with the variability in SST in individual water bodies of this ocean?

The analysis of the relationships was carried out in two time horizons, namely, asynchronous relationships, in which the SST series (1900–2017) was 1 year ahead of the SD_{13S} series (1901–2018), and synchronous relationships, in which the series of annual values of SST and SD_{13S} began in the same year, 1901.

The positive correlation of the SD_{13S} suggests that in the years with an increase in the value of the SD_{13S}, the variable SD may also increase along the western and northern coasts of the European continent. In this case, which cannot be excluded, more solar energy will reach the sea surface, and the SST in the water bodies of the North Atlantic off the coast of Europe will be higher. Thus, there will be a positive correlation between SD_{13S} and SST in these water bodies, and the variability in SD_{13S} will be the cause of the synchronously relationship.

In asynchronous analysis, where SST changes are 1 year ahead of SD_{13S} changes (Fig. 4), a dependency is detected in which the action of the cause is ahead of the effect in time. In such a situation, even in the water bodies near the shores of Europe, there may not be a situation in which the increase in SST in the preceding year (k-1) is a result of increased SD (SD_{13S}) taking place a year later (in year k).

The spatial distribution of asynchronous relationships between the variability in the SST in the North Atlantic (1900–2017), which is 1 year ahead of the change in the SD (1901–2018), is presented in Figure 5, while that of synchronous relationships (SST and SD_{13S} 1901–2018) is shown in Figure 6. The presented maps of the spatial distribution of the correlation coefficients between SST from year (k-1) and year (k) with SD_{13S}, considering the low spatial resolution of SST (10°ϕ x 10°λ), reveal only the most general features of this distribution, without detecting the points where the maxima and minima of the strength of the relationships actually occur, or may occur.

In the case of correlations where the SST variability is 1 year ahead of the SD_{13S} variability and PC1 (Fig. 5), it can be seen that positive correlations occur over the entire surface of the North Atlantic at latitudes from 20 to 70°N, while in the latitude zone from 30°N to 70°N, they are significant. Weak (0.2–0.3) and moderate (0.3–0.5) correlations predominate. An exception is the water body extending in the vicinity of latitude ~50°N between 40°W and 30°W, lying in the centre of the North Atlantic cyclonic circulation, where these correlations are very weak (r <0.2, p > 0.05) and statistically insignificant. The strongest relationships between SST and SD_{13S} of moderate strength create separate foci, which are located in three water bodies that are significantly far away from each other.

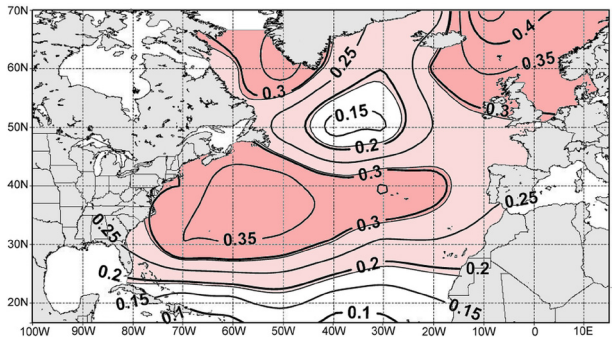

Fig. 5. Distribution of asynchronous correlation coefficients between the annual sea surface temperature SST (1900–2017) in the North Atlantic and sunshine duration SD_{13S} in the years 1901–2018. Dark pink colour denotes correlations that are highly statistically significant (p <0.001) and light pink colour denotes correlations that are statistically significant (p <0.05).

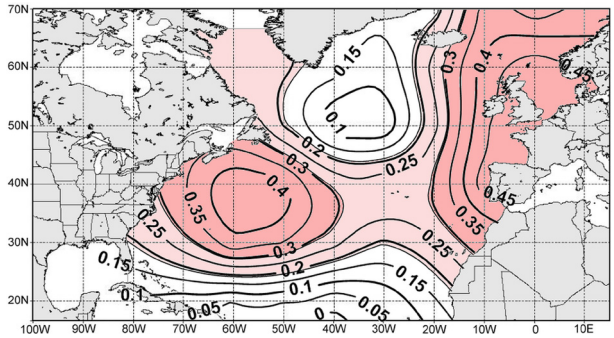

Fig. 6. Distribution of synchronous correlation coefficients between the annual sea surface temperature SST (1901–2018) in the North Atlantic and sunshine duration SD_{13S} in the years 1901–2018. Designations as in Figure 5.

The first water body is located in the NE part of the North Atlantic, in the southern and central parts of the Norwegian Sea (60°–70°N, 10°W–10°E), west of the coast of Norway (Fig. 5). It is a water body through which the waters of the warm North Atlantic and Atlantic-Norwegian currents flow, and the thermal relations of which are very strongly regulated by the variable amount of heat transported from lower latitudes along with the Atlantic water by NA THC. There are SST changes there that take place with a 3- to 6-year delay in relation to the changes in the value of the DG_{3L} index (max. SST correlation in the grid [60W, 10°W] with DG_{3L}(k-4); r = 0.72). The maximum values of the correlation coefficient between SST in this water body and SD_{13S}, which will take place in the following year, are 0.49 (grid 70°N, 10°W).

The second water body is located in the area SW of the southern tip of Greenland (~60°N, 50°W). It lies in the beginning part of the warm West Greenland Current, the temperature changes of which are regulated by two factors, namely, in the same year, the variability in the winter North Atlantic Oscillation NAO (r = –0.25) and the variability in the NA THC intensity (DG_{3L} index) from two to five years ago (correlation of SST with DG_{3L}(k-4) equal to 0.59). The value of the correlation coefficient between the annual SST in this grid (60°N, 50°W) and SD_{13S} is equal to 0.40 ($p << 0.001$).

The third, largest, of the water bodies lies in the western part of the tropical Atlantic at latitudes 30–40°N, with its centre between 60°W and 40°W (Fig. 5). The southern part of this water body is occupied by the very warm and highly saline Sargasso Sea water, and its northern part (from ~39°N) is occupied by the Gulf Stream. The maximum strength of the correlation between SST and SD_{13S} in the following year is located in the water body with the coordinates of ~40°N, in the vicinity of 60–50°W, and reaches the value of r = ~0.39 ($p << 0.001$). It is from this region of the North Atlantic that SST values are taken, from which the value of the DG_{3L} index, characterising the NA THC intensity, is then calculated. The annual variability in SST in the vicinity of 40°N, 50–60°W occurs synchronously with changes in the DG_{3L} index (r ranging from 0.75 to 0.85).

Synchronous correlations between SST and SD_{13S} (Fig. 6) reveal a spatial distribution of significant correlations between the two variables very similar to asynchronous correlations. The strength of the relationship between SST and SD_{13S} in the water bodies lying at a latitude of 70°N decreases, but clearly increases (r to 0.48) in the water bodies lying at a latitude of 60°N and situated south of them, adjacent to the coasts of Western Europe. The reason for the increase in correlation coefficients in these water bodies may be the aforementioned relationship between SST and SD_{13S}, caused by the increase in the SD over the coastal areas of Europe.

The area of occurrence of weak and insignificant correlations within the circle of the North Atlantic cyclonic circulation North Atlantic Subpolar Gyre expands and covers the waters in the vicinity of 50–60°N, 40–30°W. Significant

correlations in the initial section of the West Greenland Current also weaken, standing on the verge of statistical significance.

The synchronous correlations between SST on the border of tropical and subtropical waters in the western part of the North Atlantic (40°N, 60–50°W) slightly strengthen in relation to asynchronous correlations, explaining the approximately 17–19% SD_{13S} variances in the years 1901–2018. This water body is located 3,800–4,600 km from the coast of Europe (Iberian Peninsula), and it is difficult to imagine that changes of SD_{13S} could have a direct impact on the annual variability in SST in this body of water.

This allows us to conclude that changes in the SST in the western part of the tropical and subtropical North Atlantic have an impact, both asynchronous and synchronous, on the formation of SD variability over Europe. Owing to the size of the area of this water body and its distance from Europe, it can be assumed that it is the most important area of the North Atlantic, the variability in the thermal state of which regulates the SD over Europe.

A more detailed analysis of the relationship between SST and SD_{13S} in this water body makes it possible to find that the inter-year variability in SST is reproduced to a small extent by the same variability in SD_{13S} (Fig. 7). In the course of both variables, there is a time discrepancy in the occurrence of local minima and maxima within ±2 years, but there are also periods of several years in which the phases of the courses are reversed (e.g. 1946–1952). There are also no more tight relationships between the amplitudes of both courses. These factors affect the reduction of the value of the correlation coefficient between both courses, indicating the action of processes with strong inertia in the formation of the relationship between both courses, for which the adopted time measure (year) is too short for a clearer relationship to be determined. Nevertheless, the inter-year changes in the annual average SST at 40°N calculated from the SST in 50 and 60°W grids, without any filtering of the courses, explain ~20% of the SD_{13S} variance in a synchronous relationship. The equalisation of both courses, with only a 3-point moving average, raises the value of the correlation coefficient between them to 0.61 (n = 116, p << 0.001).

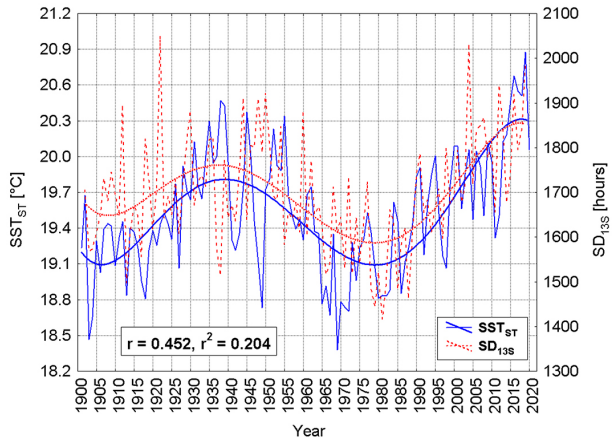

Fig. 7. Course of the average annual SST (SST_{ST}) from grids [40°N, 50°W] and [40°N, 60°W] and SD_{13S}. Bold solid lines – fitting with a 5th-degree polynomial to empirical courses. SD, sunshine duration; SST, sea surface temperature.

A clearly better consistency of both courses is visible when their long-term components are analysed. The fitting of 5th-degree polynomials to both courses shows a very good consistency in the function of time; the average decreases (increases) in the annual SST correspond to the average decreases (increases) in the annual SD over Europe. Both even courses are very strongly and highly significantly correlated with each other (Fig. 7).

This part of the analysis reveals that the spatial distribution of SST in the North Atlantic shows both asynchronous and synchronous relationships with the average annual total SD over Europe. The variability in SST in individual water bodies shows the strength of relationships with SD_{13S} that varies in space, which explains the very weak relationship of this variable with the AMO index that characterises the thermal condition of the entire surface of the North Atlantic. While in the water bodies of the North Atlantic, located on the northern and western coasts of Europe, the SST may change owing to changes in the SD over Europe, and it is difficult, in this case, to clearly indicate what is the cause and what is the result in synchronous correlations, the changes in the SST in the tropical and subtropical areas of the North Atlantic Ocean (30–40°N, 60–50°W), resulting in consistent changes in the SD over Europe, indicate that the most important cause of changes in SD_{13S} is the SST changes in these very water bodies.

Discussion of the results and conclusions

The presented results of the analyses clearly show that there are relationships between the thermal condition of the North Atlantic and the average annual total SD over Europe, which can be consistently traced over 118 years (1901–2018). This makes it possible to conclude that these relationships are stable, and their existence recorded in the years 1951–2018 (Marsz et al. 2022) was not the only case of their occurrence.

In periods when the NA THC phase is positive and SST increases (the state of the warm North Atlantic in the western part of tropical and subtropical waters and in the temperate and subpolar zones in its NE part), the SD over Europe becomes higher than average, that is a period of brightening occurs. In periods when the NA THC phase is negative and SST decreases (the state of the cool North Atlantic in the same waters), the SD over Europe drops below its average values, which corresponds to the periods of dimming. Long-term changes in SST in tropical and subtropical waters in the western part of the North Atlantic, in the vicinity of 30–40°N, 60–50°W, have the strongest impact on changes in the SD in Europe.

As a result, the following question arises: What is the mechanism of the teleconnection-like relationship between the variable NA THC intensity and the associated multi-decadal variability in SST (Fig. 7) and SD over Europe?

In the work of Marsz et al. (2022), it has been shown that the influence of changes in THC NA intensity on the SD is realised by controlling the mid-tropospheric circulation (level 500 hPa) in the Atlantic-Eurasian circulation sector. A special role in controlling the variability in the mid-tropospheric circulation is played by the variability in the meridional gradients of the ocean surface temperature, which is strongly dependent on the spatial distribution of heat resources in the waters and, therefore, to a large extent, on the spatial distribution of the SST at low latitudes.

Depending on whether the heat resources in the waters of the tropical and subtropical zones are larger or smaller than the average, and thus on the increases or decreases in the meridional gradients of the SST, changes occur in the wavenumber of long waves travelling in this circulation sector and in the average position of the upper ridges and upper troughs over the eastern North Atlantic and Eurasia, to approximately 100–130°E.

In periods when heat resources in tropical and subtropical waters are greater than the average, the frequency of long waves with wavenumber 4, which are an equivalent of macrotype W according to the Wangengejm–Girs classification (Wangengejm 1952, Girs 1964), increases in this circulation sector. What is characteristic for this macrotype is the occurrence of an extensive upper trough over the western and central North Atlantic with its axis at ~40–35° W, and over the eastern North Atlantic and Western Europe of a stretched upper ridge of a not very large amplitude, the axis of which is located along a longitude of ~5–10°E.

During periods when ocean heat transport to the north weakens and the ocean heat resources are lower than average, the frequency of long waves with wavenumber 5 increases. The equivalent of waves of this length are macrotypes E and C according to the Wangengejm–Girs classification. In the average long-term course, the frequency of macrotype E definitely dominates over the frequency of macrotype C (~2:1). With the decrease in the annual frequency of macrotype W, this leads to a significant increase in the frequency of macrotype E in such periods. With the occurrence of macrotype E over the eastern part of the North Atlantic and Western Europe, there is a strongly extended upper trough reaching the southern shores of the Mediterranean Sea with an axis located at a longitude of ~5–10°E, and an equally strongly marked upper ridge over Eastern Europe (with an axis at ~40–50°E), reaching latitudes of 75–80°N.

Depending on the changes in the frequency of macrotypes W and E in relation to their long-term average frequency, the SD over European stations changes; along with the increase in the frequency of macrotype W, the frequency of macrotype E must decrease, and the SD over Europe increases.

The annual total SD over a given area are strongly related to changes in the average annual geopotential height over that area. The reason for the occurrence of such relationships is relatively simple, but their explanation should be related to

the processes of the synoptic scale. The occurrence over a given area of the upper trough or upper ridge is recorded as changes in height h500. The h500 area above the upper ridge lies higher than the upper trough, and thus, the average annual height of the geopotential above a given area depends on the frequency of passage of the upper ridges and upper troughs over it. The more the cases of upper ridges occurring over a given area during the year, the higher the average annual isobaric area of 500 hPa. Thus, the increase in the annual height h500 over Western Europe signals an increase in the frequency of macrotype W this year and a decrease in the frequency of macrotype E.

To the east of the axis of the upper ridge, in the lower troposphere, lower anticyclonic systems (Fortak 1971) are formed, in which anticyclonic types of intra-mass weather with reduced layer cloud cover predominate, especially at the low and the middle level. Weather of this kind is conducive to an increase in the SD. This is particularly important in the warm half-year, when the day is long; the more often anticyclonic weather occurs, the higher the total annual SD becomes.

The increase in the frequency of anticyclonic weather over an area reduces the percentage of the time of the year in which cyclonic weather occurs above it. Amongst cyclonic weathers, the frontal weather, which is characterised by the presence of extensive zones of low and medium layer cloud cover strongly limiting SD, represents a significant percentage.

Thus, with changes in the height of the geopotential above Western and Central Europe and the corresponding changes in the frequency of macrotypes W and E during the year, it is not so much the value of the total cloud cover (N) as the cloud cover structure that must change. With an increased frequency of macrotype W, the frequency of anticyclonic weather increases and the share of stratiform clouds (*Altostratus*, *Nimbostratus*, *Stratus*), typical for frontal weather, in the cloud cover structure decreases, and the share of convective clouds (*Cumulus*, *Cumulonimbus*) and possibly high clouds (*Cirrus*, *Cirrocumulus*, *Cirrostratus*) increases.

Such a diagram of changes in the cloud cover structure, showing connections with changes in the NA THC phases and circulation epochs, is confirmed by the results of research on cloud cover changes carried out in Poland. Analysing the course of the cloud cover in Krakow in the years 1906–2000, Matuszko and Węglarczyk (2018) found a decrease in the frequency of *Nimbostratus* and *Stratus* clouds in the last four decades of that period (1961–2000). Żmudzka (2007), who found that a decrease in the frequency of low- and medium-level stratiform clouds is accompanied by an increase in the frequency of high-level clouds and also pointed to such changes in the cloud cover structure over Poland in the years 1966–2000. The results of the research by Żmudzka (2007) also indicate quite a clear linking of changes in cloud cover to the boundaries of circulation epochs. Similarly, analysing the trends of changes in cloud types in the period 1951–2000 in Łódź, Wibig (2008) detected the occurrence of negative trends in the number of occurrences of *Stratus* and *Nimbostratus* clouds and, in the course of the number of occurrences of *Altostratus* clouds, the occurrence of a negative sub-trend in the years ~1980–2000. A recent detailed study by Matuszko et al. (2022) of the changes in the cloud cover over Poland, covering the period 1971–2020, indicates a clear increase in the SD during that period and a simultaneous decrease in cloud cover created by *Stratus*, *Nimbostratus*, and *Altostratus* clouds. On an annual scale, this decrease is statistically significant. In the cloud cover structure, the stratiform clouds of the low and medium levels are replaced by vertical clouds (*Cumulus*, *Cumulonimbus*), the positive annual trend of which is also statistically significant, and the value of this trend is close to the value of the negative trend of stratiform clouds.

These works cover, in their time interval, the transition from circulation epochs E+C and E to epoch W and, in relation to the NA THC phases, the final period of the positive NA THC phase (1927–1963), the period of the negative NA THC phase (1964–1988), and the last, positive NA THC phase (1989–....) which has lasted to date. Thus, changes in the nature of cloud cover during the transition from the negative NA THC phase (1964–1988) to the positive NA THC phase, in which a strong positive trend is marked (after 1988; Fig. 1), should show trends with exactly these signs. Since the macrotypes of the mid-tropospheric circulation according to the Wangengejm–Girs classification are nothing other than long waves (Rossby waves) with a

specific, characteristic location of the upper ridges and upper troughs, the change in the frequency of macrotypes in individual NA THC phases or circulation epochs entails changes in the SD.

The following examples illustrating the relationships discussed previously do not cover the entire period under consideration (1901–2018), but only the years 1949–2018, as the data about height h500 from the National Centers for Environmental / National Center for Atmospheric Research (NCEP/NCAR) Reanalysis begin with the year 1949. The European stations, the data of which were used to calculate the SD_{13S} variable, lie approximately between 45 and 55°N and 5°W and 20°E. From the taken values of h500, 3 latitudinal profiles were created for 45°, 50° and 55°N across Europe (from 10°W to 60°E), with a horizontal resolution of 5°λ. The values of the total annual SD from the considered stations (variable SD_{13S}) were correlated with h500 in each of the points of these profiles (Fig. 8).

The distribution of correlation coefficients between h500 and SD_{13S}, as shown in Figure 8, indicates the presence of strong and highly significant correlations between SD and geopotential height, where the local maxima of the curves are, obviously, located at longitudes corresponding to the location of the set of 13 stations (~5–15°E). However, it should be noted that regardless of latitude, these maxima remain in the same longitude range.

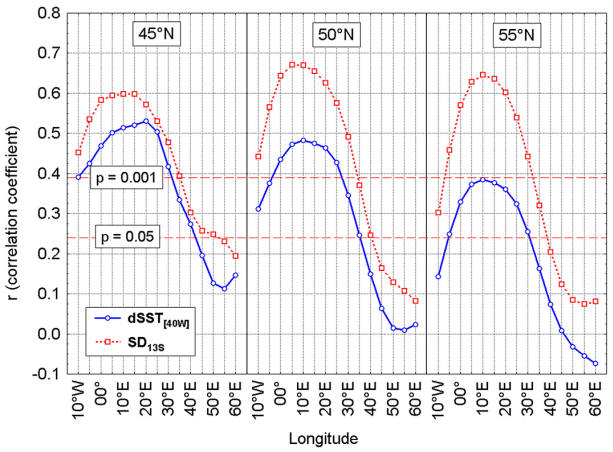

Fig. 8. Linear correlation coefficients (r) between SD_{13S} and the meridional SST gradient in the North Atlantic between 30 and 60°N to 40°W (average ϕ = 45°N; $dSST_{[40W]}$) and the geopotential height at h500 at 45°, 50° and 55°N. Significance levels of correlation (p) are marked. Period of analysis 1949–2018. SD, sunshine duration; SST, sea surface temperature.

The meridional SST gradient between 30°N and 60°N at 40°W ($dSST_{[40W]}$) describes the annual temperature difference between tropical waters and subpolar waters in the middle of the North Atlantic ($dSST_{[40W]}$ = SST [30°N, 40°W] – SST [60°N, 40°W]). The warmer the waters in the tropics (30°N) than the temperature of the waters in the North Atlantic subpolar zone (60°N), the greater the gradient. It is on the value of this gradient that the meridian temperature gradient in the central troposphere (on average ~45°N) depends, which determines the velocity of the zonal wind and the stability conditions for long waves (Fortak 1971).

The course of the correlation coefficients between $dSST_{[40W]}$ and h500, as shown in Figure 8, reproduces the waveform in the geopotential area between 10°W and 60°E. The maximum value of the correlation coefficient curve is between 10°E (at 50° and 55°E) and 20°E (at 45°N), which indicates that the axis of the upper ridge is located, on average, on these longitudes. At a latitude of 50°N, the axis of the upper ridge is located at 10°E, while the axis of the upper trough of the same wave is located at 55°E. This indicates that the wavelength is 90°, that is the wavenumber of the presented wave is 4. This allows us to identify the long wave presented in Figure 8, as macrotype W according to the Wangengejm–Girs classification.

A positive correlation coefficient between the meridional SST gradient and h500 indicates that as the value of the meridional SST gradient increases in the middle parts of the North Atlantic, and thus along with the increase in SST in the Atlantic tropics, the frequency of macrotype W increases, and with it, as well as the height of the geopotential at the level of 500 hPa over Europe, with a maximum longitude of 10–20°E. Thus, the annual SD over Europe also increases, and the consistency of the maxima of the strength of SD relationships with h500 and the maxima of the strength of relationships of h500 with $dSST_{[40W]}$ is not accidental.

A similar analysis of the correlations between h500 on the latitudinal profile across Europe and variables DG_{3L} and SST_{ST} (Fig. 9), limited to a latitude of 50°N, also reveals the wave course of the relationship, with a clearly defined maximum of its strength at 30°E. The same, positive sign of the correlation coefficient is preserved, clearly

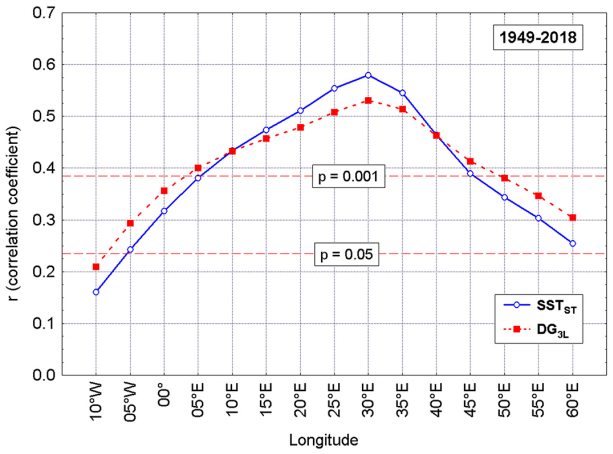

Fig. 9. Distribution of the values of the correlation coefficients between the height of the geopotential 500 hPa at 50°N (from 10°W to 60° E) and the DG_{3L} index and the annual mean SST at 40°N, 60–50°W (variable SST_{ST}). Significance levels (p = 0.001 and p = 0.05) are marked. SST, sea surface temperature.

indicating that with the increase in the value of DG_{3L} and SST_{ST}, the height of the geopotential increases. The maximum values of the correlation coefficients are slightly higher here than in the case of the h500 correlation with the meridional SST gradient at 40°W, but it seems important to indicate that in the zone between ~5°E and ~45°E (within ~2,860 km), this relationship is highly significant. Thus, as NA THC intensity increases and SST increases in the tropics and subtropics in the western North Atlantic, there will be an increase, albeit to a different extent, in the height of the geopotential and SD over virtually all of Europe.

The asymmetry of the slope of the curves with respect to the maximum point can be considered a certain peculiarity of the relationship presented in Figure 9, that is the increasing r values greater than r = 0.4 extend approximately from 5°E to 30°E, while the decreasing from 30°E to 45°E. This shows that with the same changes in SST and DG_{3L} index, the average increase in height h500 (and SD) over Western Europe and Central Europe (west of 30°E) is greater than that east of 30°E, where height h500 and SD decrease approximately twice as fast.

The presented dependencies explain that the occurrence of long-term variability in the SD over Europe, manifested in the occurrence of successive phases of dimming and brightening, can be explained without resorting to changes in the concentration of volcanic and anthropogenic aerosols in the atmosphere. Over the course of 118 years, the course of changes in the annual SD over Europe shows consistency in time with the changes in the thermal condition of the North Atlantic, which are controlled by the surface component of the thermohaline circulation. This consistency of changes in time of both amounts can be relatively easily explained by outlining the chain of processes successively influencing the course of the next process:

changes of NA THC phases → changes in the amount of heat transported north from the Atlantic tropics → changes in the spatial distribution of heat resources in the North Atlantic waters → changes in meridional SST gradients in the North Atlantic → changes in the location and spatial distribution of heat flows from the ocean to the atmosphere → changes in the nature of the mid-tropospheric circulation in the Atlantic-Eurasian circulation sector → changes in the frequency of macrotypes W and E → changes in the weather structure (share of anticyclonic and cyclonic weather) → changes in cloud cover structure → changes in sunshine duration.

However, the interrelationships in this chain of processes are so strong that the last element of this chain (the effect – changes in SD) shows a significant correlation with the first element of this chain, which is the primary cause that triggers the cycle of changes (changes of NA THC phases).

The NA THC is widely regarded as a factor regulating the course of climatic processes in the vicinity of the North Atlantic (e.g. Dong, Sutton 2003, Sutton, Hodson 2005, 2007, Alexander et al. 2014, Jackson et al. 2015), in the northern hemisphere (e.g. Knight et al. 2005, Semenov et al. 2010, Wyatt et al. 2012, Buckley, Marshall 2015), and quite often also as a factor regulating climate change on a global scale (e.g. Chylek et al. 2014, 2016, Lyu, Yu 2017). In such a situation, the same factor as the Atlantic THC also regulates one of the most important climatic elements for Europe's heat balance, which is the annual total SD.

However, the ultimate primary cause of changes in the SD over Europe, whether these are changes in NA THC or the long-term changes in the concentration of aerosols in the atmosphere, mentioned at the beginning of this article, is somewhat debatable. The problem is whether the long-term variability in the thermal condition

of the North Atlantic is the result of natural variability resulting from the internal dynamics of the climate system, or is the result of changes in the concentration of aerosols in the atmosphere.

A number of climatologists assume that long-term changes in the SST in the North Atlantic, including changes in AMO, occur as a result of changes in the concentration of aerosols in the atmosphere, which themselves or in cooperation with cloud cover changing in step with changes in aerosol concentrations change the inflow of solar radiation to the ocean's surface (e.g. Mann, Emanuel 2006, Booth et al. 2012, Birkel et al. 2018, Qin et al. 2020). Recently, Mann et al. (2020, 2021), based on the results of modelling, have put forward the thesis that the long-term variability in the thermal condition of the North Atlantic, manifested in the occurrence of AMO, is only the effect of forcing by the variability in the concentrations of volcanic and anthropogenic aerosols, and that the participation of the internal dynamics of the system in the formation of the long-term variability in SST, as such, does not exist. Adopting this point of view, the described changes in the SD would have their primary cause in the changes in the concentration of aerosols, regardless of the share of the ocean and atmospheric circulation in the formation of their variability.

A polemic with the views of Mann and Emanuel (2006) was undertaken by Zhang (2007) who presented arguments clearly pointing to AMOC as the main cause of the long-term variability in the thermal condition of the North Atlantic Ocean. He showed the existence of long-term anti-correlations between SST anomalies in the tropical North Atlantic and water temperature anomalies at a depth of 400 m, as well as a shift in time between the course of the SST anomalies between the tropical and subpolar North Atlantic (Fig. 1A and 1C in the cited work by Zhang). Both of these phenomena are physically impossible to explain by the effect of changes in the amount of radiation reaching the ocean's surface, and thus regulating changes in SST by changes in the concentrations of aerosols, while clearly indicating the action of the ocean circulation in their formation (AMOC). AMO and AMOC are manifestations of the action of the NA THC, which, according to the commonly accepted opinion, is the result of the natural, internal variability in the system (e.g. Trenberth, Shea 2006, Grossmann, Klotzbach 2009, Knight 2009, Hartmann 2016, Zhang et al. 2019). In view of the appearance of further studies presenting the results of modelling, indicating changes in aerosol concentration as the cause of long-term variability in SST in the North Atlantic, a number of studies have appeared pointing to the lack of justification for such results and the inconsistency of the modelling results with the materials from *in situ* observations. The most important of them, specifically devoted to the role of aerosols in the formation of the long-term variability in the thermal condition of the North Atlantic, was the work of Zhang et al. (2013), in which a number of pieces of evidence were presented to indicate that there is no basis for formulating this type of hypothesis. In Mann et al. (2020), neither the work of Zhang (2007) nor the work of Zhang et al. (2013) was referred to, ignoring the arguments presented there that indicate the functioning of internal variability and its role in the formation of long-term changes in the thermal condition of the North Atlantic. Also, Stanhill et al. (2014) and Dübal and Vahrenholt (2021) indicated that the role of changes in aerosol concentration in shaping changes in SD is not at all obvious. Similarly, Veretenenko and Ogurtsov (2016) showed that changes in cloud cover created by low clouds in moderate latitudes are closely related to changes in the frequency of cyclones and their frontal cloud zones.

The mechanisms of THC NA functioning are known and indicate that they are the result of the internal variability in the ocean–atmosphere system. SST changes occur not only because of changes in the amount of radiation reaching the ocean's surface but also due to the meridonal oceanic heat transport.

Adopting this point of view, it is the long-term changes in the thermal condition of the North Atlantic, and not the changes in the concentration of aerosols, that would be the primary cause of the long-term changes in the SD over Europe presented here.

Acknowledgments

Translation/proofreading of this publication has been supported by a grant from the Faculty of Geography and Geology under the Strategic Programme Excellence Initiative at Jagiellonian

University. The authors thank the anonymous reviewers for contributing to the improvement of our article.

Author's contribution

Andrzej Marsz: Conceptualization; methodology; writing-review & editing; Anna Styszyńska: Visualization; writing-original draft; writing-review & editing; Dorota Matuszko: Project administration; supervision; writing-review & editing.

References

Alexander M.A., Kilbourne H., Nye J.A., 2014. Climate variability during warm and cold phases of the Atlantic multidecadal oscillation (AMO) 1871–2008. Journal *of Marine* Systems 133: 14–26. DOI 10.1016/j.jmarsys.2013.07.017.

Bartoszek K., Matuszko D., Węglarczyk S., 2021. Trends in sunshine duration in Poland (1971–2018). *International Journal of Climatology* 41(1): 73–91. DOI 10.1002/joc.6609.

Birkel S.D., Mayewski P.A., Maasch K.A., Kurbatov A.V., Lyon B., 2018. Evidence for a volcanic underpinning of the Atlantic multidecadal oscillation. *npj Climate and Atmospheric Science* 1, 24. DOI 10.1038/s41612-018-0036-6.

Booth B.B.B., Dunstone N.J., Halloran P.R., Andrews T., Bellouin N., 2012. Aerosols implicated as a prime driver if twentiech-century North Atlantic climate variability. *Nature* 484: 228–232.

Brázdil R., Flocas A., Sahsamanoglou H., 1994. Fluctuation of sunshine duration in central and South-Eastern Europe. *International Journal of Climatology* 14(9): 1017–1034. DOI 10.1002/joc.3370140907.

Bryś K., 2013. *Dynamika bilansu radiacyjnego murawy oraz powierzchni nieporośniętej*. Monografie CLXII, Wydawnictwo Uniwersytetu Przyrodniczego we Wrocławiu, Wrocław.

Buckley M.W., Marshall J., 2015. Observations, inferences, and mechanism of the Atlantic meridional overturning circulation: A review. *Reviews of* Geophysics 54(1): 5–63. DOI 10.1002/2015RG000493.

Chylek P., Klett J.D., Dubley M.K., Hengartner N., 2016. The role of Atlantic multidecadal oscillation in the global mean temperature variability. *Climate Dynamics* 47: 3271–3279. DOI 10.1007/s00382-016-3025-7.

Chylek P., Klett J.D., Lesins G., Dubley M.K., Hengartner N., 2014. The Atlantic multidecadal oscillation is a dominant factor of oceanic influence on climate. *Geophysical Research Letters* 41(5): 1689–1697. DOI 10.1002/2014GL059274.

Delworth T.L., Greatbatch R.J., 2000. Multidecadal thermohaline circulation variability driven by atmosphere surface flux forcing. *Journal of Climate* 13(9): 1481–1495. DOI 10.1175/1520-0442(2000)013<1481:MTCVDB>2.0.CO;2.

Dima M., Lohmann G., 2007. A hemispheric mechanism for the Atlantic multidecadal oscillation. *Journal of Climate* 20(11): 2706–2719. DOI 10.1175/JCLI4174.1.

Dong B., Sutton R., 2003. Variability of Atlantic Ocean heat transport and its effects on the atmosphere. *Annals of Geophysics* 46(1): 87–97. DOI 10.4401/ag-3391.

Dong B., Sutton R.T., 2005. Mechanism of interdecadal thermohaline circulation variability in a coupled ocean-atmosphere GCM. *Journal of Climate* 18(8): 1117–1135. DOI 10.1175/JCLI3328.1.

Dübal H.R., Vahrenholt F., 2021. Radiative energy flux variation from 2001–2020. *Atmosphere* 12: 1297. DOI 10.3390/atmos12101297.

Enfield D.B., Mestas-Nunez A.M., Trimble P.J., 2001. The Atlantic multidecadal oscillation and its relationship to rainfall and river flows in the continental US. *Geophysical Research Letters* 28(10): 2077–2080. DOI 10.1029/2000GL012745.

Fortak H., 1971. *Meteorologie* Deutsche Buch-Gemainschaft Berlin, Darmstadt, Wien.

Girs A.A., 1964. O sozdanii edinoi klassifikacii makrosinopticheskikh processov severnogo polushariya. *Meteorologya i Gidrologiya* 4: 43–47.

Girs A.A., Kondratovich K.V., 1978. *Metody dolgosrochnykh prognozov pogody*. Girometeoizdat, Leningrad.

Grossmann I., Klotzbach P.J., 2009. A review of North Atlantic modes of natural variability and their driving mechanism. *Journal of Geophysical Research* 114(D24): 107. DOI 10.1029/2009JD012728.

Hartmann D.L., 2016. *Global physical climatology, Second Edition*. Elsevier. Amsterdam, Netherlands. DOI 10.1016/C2009-0-00030-0.

Hill T., Lewicki P., 2007. *STATISTICS: Methods and Applications*. StatSoft, Tulsa, OK. Online: www.statsoft.com/textbook/stathome.html (accessed on October 30, 2022)

Jackson I.C., Kahana R., Graham T., Ringer M.A., Woollings T., Mecking J.V., Wood R.A., 2015. Global and European climate impacts of a slowdown of the AMOC in a high resolution GCM. *Climate Dynamics* 45: 3299–3316. DOI 10.1007/s00382-015-2540-2.

Kalnay E., Kanamsitu M., Kistler R., Collins W., Deaven D., Gandin L., Iredell M., Saha S., Withe G., Woolen J., Zhu Y., Chelliah M., Ebisuzaki W., Higgins W., Jankowiak J., Mo C.K., Ropelewski C., Wang J., Leetmaa A., Reynolds R., Jenne R., Joseph D., 1996. The NCEP/NCAR 40-Year reanalysis project. *Biulletin of the American Meteorological Society* 77(3): 437–471.

Kerr R.A., 2000. A North Atlantic climate pacemaker for the centuries. *Science* 288(5473): 1984–1985. DOI 10.1126/science.288.5473.1984.

Knight J.R., Allan R.J., Folland C.K., Vellinga M., Mann M.E., 2005. A signature of peristent natural thermohaline circulation cycles in observed climate. *Geophysical Research Letters* 32(20): L20708. DOI 10.1029/2005GL024233.

Knight R.J., 2009. The Atlantic multidecadal oscillation inferred from the forced climate response in coupled general circulation models. *Journal of Climate* 22(7): 1610–1625. DOI 10.1175/2008JCLI2628.1.

Kushnir Y., 1994. Interdecadal variations in North Atlantic Sea surface temperature and associated atmospheric conditions. *Journal of Climate* 7(1): 141–157. DOI 10.1175/1520-0442(1994)007<0141:IVINAS>2.0.CO;2.

Liepert B.G., 2002. Observed reductions of surface solar radiation at sites in the United States and worldwide from 1961 to 1990. *Geophysical Research Letters* 29(10): 1421. DOI 10.1029/2002GL014910.

Lyu K., Yu J.Y., 2017. Climate impacts of the Atlantic multidecadal oscillation simulated in the CIMP5 models: A re-evaluation based on a revised index. *Geophysical Research Letters* 44(8): 3867–3876. DOI 10.1002/2017GL072681.

Manara V., Beltrano M.C., Brunetti M., Maugeri M., Sanchez-Lorenzo A., Simolo C., Sorrenti S., 2015. Sunshine duration variability and trends in Italy from homogenized instrumental time series (1936–2013). *Journal of Geophysical Research* 120(9): 3622–3641. DOI 10.1002/2014JD022560.

Mann M.E., Emanuel K.A., 2006. Atlantic hurricane trends linked to climate change. *Eos. Transactions, American Geophysical Union* 87(24): 233–244. DOI 10.1029/2006EO240001.

Mann M.E., Steinman B.A., Brouillette D.J., Miller S.K., 2021. Multidecadal climate oscillations during the past millennium driven by volcanic forcing. Science 371(6533): 1014–1019. DOI 10.1126/science.abc5810.

Mann M.E., Steinman B.A., Miller S.K., 2020. Absence of internal multidecadal and interdecadal oscillations in climate model simulations. Nature Communications 11: 49. DOI 10.1038/s41467-019-13823-w.

Marsz A.A., 2015. Model zmian powierzchni lodów morskich Arktyki (1979–2013) – zmienne sterujące w modelu minimalistycznym" i ich wymowa klimatyczna. *Problemy Klimatologii Polarnej* 25: 249–334.

Marsz A.A., Matuszko D., Styszyńska A., 2022. The thermal state of the North Atlantic and macro-circulation conditions in the Atlantic-European sector, and changes in sunshine duration in Central Europe. *International Journal of Climatology* 42(2): 748–761. DOI 10.1002/joc.7270.

Marsz A.A., Styszyńska A., Bryś K., Bryś T., 2021. Role of internal variability of climate system in increase of air temperature in Wrocław (Poland) in the years 1951–2018. *Quaestiones Geographicae* 40(3): 109–124. DOI 10.2478/quageo-2021-0027.

Matuszko D., Bartoszek K., Soroka J., 2022. Long-term variability of cloud cover in Poland (1971–2020). *Atmospheric Research* 283: 106028. DOI 10.1016/j.atmosres.2022.106028.

Matuszko D., Węglarczyk S., 2018. Long-term variability of the cloud amount and cloud genera and their relationship with circulation (Kraków, Poland). *International Journal of Climatology* 38(51): 1205–1220. DOI 10.1002/joc.5445.

Norris J.R., Wild M., 2007. Trends in aerosol radiative effects over Europe inferred from observed cloud cover solar 'dimming' and solar 'brightening'. *Journal of Geophysical Research, Atmospheres* 112: D82014. DOI 10.1029/2006JD007794.

Qin M., Dai A., Hua W., 2020. Aerosol-forced multidecadal variations across all ocean basins in models and observations since 1920. *Science Advances* 6(29): eabb0425. DOI 10.1126/sciadv.abb0425.

Ruckstuhl C H., Norris J.R., 2009. How do aerosol histories affect solar "dimming" and "brightening" over Europe? IPCC-AR4 models versus observations. *Journal of Geophysical Research*, *Atmosphere* 114: D00D04. DOI 10.1029/2008JD011066.

Sanchez-Lorenzo A., Calbó J., Brunetti M., Deser C., 2009. Dimming/brightening over the Iberian Peninsula: Trends in sunshine duration and cloud cover and their relations with atmospheric circulation. *Journal of Geophysical Research, Atmosphere* 114(D10): D00D09. DOI 10.1029/2008JD011394.

Sanchez-Lorenzo A., Calbó J., Martin-Vide J., 2008. Spatial and temporal trends in sunshine duration over Western Europe (1938–2004). *Journal of Climate* 21(22): 6089–6098. DOI 10.1175/2008JCLI2442.1.

Semenov V.A., Latif M., Dommenget D., Keenlyside N.S., Strehz A., Martin T., Park W., 2010. The impact of North Atlantic-Arctic multidecadal variability on Northern Hemisphere surface air temperature. *Journal of Climate* 23(21): 5668–5677. DOI 10.1175/2010JCLI3347.1.

Smith T.M., Reynolds R.W., Peterson T.C., Lawrimore J., 2008. Improvements to NOAA's historical merged Land-Ocean surface temperature analysis (1880–2006). *Journal of Climate* 21(10): 2283–2296. DOI 10.1175/2007JCLI2100.1.

Stanhill G., Achiman O., Rosa R., Cohen S., 2014. The cause of solar dimming and brightening at the Earth's surface during the last half century: Evidence from measurements of sunshine duration. *Geophysical Research Letters* 119(18): 10902–10911. DOI 10.1002/2013JD021308.

Stjern C.W., Kristjansson J.E., Hansen A.W., 2009. Global dimming and global brightening – an analysis of surface radiation and cloud cover data in northern Europe. *International Journal of Climatology* 29(5): 643–653. DOI 10.1002/joc.1735.

Sutton R., Dong B., 2012. Atlantic Ocean influence on a shift in European climate in the 1990s. Nature Geoscience 5: 788–792. DOI 10.1038/ngeo1595.

Sutton R.T., Hodson D.L.R., 2005. Atlantic Ocean forcing of North American and European summer climate. *Science* 309(5731): 115–118. DOI 10.1126/science.1109496.

Sutton R.T., Hodson D.L.R., 2007. Climate response to basin-scale warming and cooling of the North Atlantic Ocean. *Journal of Climate* 20(5): 891–907. DOI 10.1175/JCLI4038.1.

Trenberth K.E., Shea D.J., 2006. Atlantic hurricanes and natural variability in 2005. *Geophysical Research Letters* 33: L12704. DOI 10.1029/2006GL026894.

Urban G., Migała K., Pawliczek P., 2018. Sunshine duration and its variability in the main ridge of the Karkonosze Mountains in relation to with atmospheric circulation. *Theoretical and Applied Climatology* 131: 1173–1189. DOI 10.1007/s00704-017-2035-7.

Veretenenko S., Ogurtsov M., 2016. Cloud cover anomalies at middle latitudes: Links to troposphere dynamics and solar variability. *Journal of Atmospheric and Solar-Terrestrial Physics* 149: 207–218. DOI 10.1016/j.jastp.2016.04.003.

Vetter T., Wechsung T., 2015. Direct aerosol effects during periods of solar dimming and brightening hidden in the regression residuals: Evidence from Potsdam measurements. *Journal of Geophysical Research Atmospheres* 120(21): 11299–11305. DOI 10.1002/2015JD023669.

Wangengejm G.Ya., 1952. Osnovy makrocirkuylacionngo metoda dolgosrochnykh meteorologicheskikh prognozov dlya Arktiki. *Trudy AANII* 34: 1–314.

Wibig J., 2008. Variability and trends in cloud characteristics in Lodz in the second half of the 20th century. *International Journal of Climatology* 28(4): 479–491. DOI 10.1002/joc.154476.

Wrzesiński D., Marsz A.A., Styszyńska A., Sobkowiak L., 2019. Effect of the North Atlantic thermohaline circulation on changes in climatic conditions and river flow in Poland. *Water* 11(8): 1622. DOI 10.3390/w11081622.

Wyatt M.G., Kravtsov S., Tsonis A.A., 2012. Atlantic mutlidecadal oscillation and Northern Hemisphere's cilmate variability. *Climate Dynamics* 38(5): 929–949. DOI 10.1007/s00382-011-1071-8.

Zhang R., 2007. Anticorrelated multidecadal variations between surface and subsurface tropical North Atlantic. Geophysical Research Letters 34(12): L12713. DOI 10.1029/2007GL030225.

Zhang R., Delworth,T., Sutton R., Hodson D.L.R., Dixon K.W., Held I.M., Kushnir Y., Marshall J.C., Ming Y., Msadek R., Robson J., Rosati A., Ting M.F., Vecchi G.A., 2013. Have aerosols caused the observed Atlantic multidecadal variability? *Journal of the Atmospheric Sciences* 70(4): 1135–1144. DOI 10.1175/JAS-D-12-0331.1.

Zhang R., Sutton R., Danabasoglu G., Kwon Y.O., Marsh R., Yager S.G., Amrhein D.E., Little C.M., 2019. A review of the role of the Atlantic meridional overturning circulation in Atlantic multidecadal variability and associated climate impacts. *Reviews of* Geophysics 57(2): 316–375. DOI 10.1029/2019RG000644.

Żmudzka E., 2007. *Variability of cloudiness over Poland and its circulation-related conditioning (1951–2000)*. Wydawnictwa Uniwersytetu Warszawskiego, Warszawa.